

## Communications

### Molecular Changes during Tensile Deformation of Single Wood Fibers Followed by Raman Microscopy

Notburga Gierlinger,<sup>\*,†</sup> Manfred Schwanninger,<sup>‡</sup> Antje Reinecke,<sup>†</sup> and Ingo Burgert<sup>†</sup>

Max-Planck-Institute of Colloids and Interfaces, Department of Biomaterials, Potsdam, Germany, and  
BOKU - University of Natural Resources and Applied Life Sciences, Department of Chemistry,  
Vienna, Austria

Received March 13, 2006; Revised Manuscript Received April 29, 2006

Raman spectra were acquired in situ during tensile straining of mechanically isolated fibers of spruce latewood. Stress-strain curves were evaluated along with band positions and intensities to monitor molecular changes due to deformation. Strong correlations ( $r = 0.99$ ) were found between the shift of the band at  $1097\text{ cm}^{-1}$  corresponding to the stretching of the cellulose ring structure and the applied stress and strain. High overall shifts ( $-6.5\text{ cm}^{-1}$ ) and shift rates ( $-6.1\text{ cm}^{-1}/\text{GPa}$ ) were observed. After the fiber failed, the band was found on its original position again, proving the elastic nature of the deformation. Additionally, a decrease in the band height ratio of the  $1127$  and  $1097\text{ cm}^{-1}$  bands was observed to go hand in hand with the straining of the fiber. This is assumed to reflect a widening of the torsion angle of the glycosidic C—O—C bonding. Thus, the  $1097\text{ cm}^{-1}$  band shift and the band height ratio enable one to follow the stretching of the cellulose at a molecular level, while the lignin bands are shown to be unaffected. Observed changes in the OH region are shown and interpreted as a weakening of the hydrogen-bonding network during straining. Future experiments on different native wood fibers with variable chemical composition and cellulose orientation and on chemically and enzymatically modified fibers will help to deepen the micromechanical understanding of plant cell walls and the associated macromolecules.

#### Introduction

Wood is a complex biocomposite, evolutionarily designed to allow trees to grow to great heights and persist for several hundred years. The wooden cell wall is composed of parallel cellulose aggregates in a matrix of lignin and hemicelluloses.<sup>1</sup> Functional characteristics of cell walls depend on fine details of their macromolecular structure and conformation and on their highly ordered architecture at scales from a few nanometers to several microns. When cell wall macromolecules are extracted into solution, as necessary for examinations with classical techniques of polysaccharide and lignin chemistry, the highly sophisticated polymer network is degraded, and “fine-structural” details are lost. By contrast, spectroscopic techniques such as

solid-state nuclear magnetic resonance (NMR), Fourier transform infrared (FTIR), and Raman microscopy allow one to study plant cell walls in the native state without prior fractionation or solubilization.<sup>2,3</sup>

Raman spectroscopy has during the last two decades developed as an important tool for nondestructive investigations of the structure and arrangement of cellulose and matrix molecules in plant cell walls, for example.<sup>2,4–9</sup> Besides, it has proven an invaluable method for evaluating molecular changes that occur in a fiber structure subjected to stress and strain. The first experiments done on monocrystalline polydiacetylene fibers<sup>10</sup> were followed by studies on polymeric fibers, for example, refs 11 and 12, and recently, various forms of cellulose fibers have been studied.<sup>13–18</sup> In cellulose fibers and cellulose composite systems (wood and paper), the intense Raman band at  $1095\text{ cm}^{-1}$  was observed to be shifted to lower wavenumbers during tensile deformation. This band corresponds to the vibration of bonds within the backbone of the cellulose molecule and is dominated by the C—O stretching motion, which is almost

\* Notburga Gierlinger, Max-Planck-Institute of Colloids and Interfaces, Department of Biomaterials, D-14424 Golm. Phone: +49-331-567 9426. Fax: +49-331-567 9402. Email: gierlinger@mpikg.mpg.de.

† Max-Planck-Institute of Colloids and Interfaces.

‡ BOKU.

parallel to the chain axis. The band shift was found to be indicative of the stress in the fibers and the shift rate invariant with stress in various cellulosic fibers (no matter what the supposed crystal structure or specific mechanical properties).<sup>13</sup> Most of the studies deal with regenerated cellulose II fibers,<sup>14–18</sup> but also flax and hemp fibers<sup>18,19</sup> as well as paper and wood have been studied.<sup>13</sup> The study on wood was done on small wood slivers using a four-point-bending setup with a collection of spectra at different strain levels.<sup>13</sup>

In this work, we used single wood fibers, which have been mechanically isolated<sup>20</sup> and thus present the native state of a single wood cell.<sup>21</sup> We aimed at tensile experiments with a controlled, continuous straining and concurrent force registration along with an acquisition of Raman spectra to monitor in situ molecular changes in the wood polymers.

### Experimental Methods

A tangential section (200  $\mu\text{m}$ ) of spruce latewood was cut on a rotary microtome (LEICA RM2255, Germany) from which single wood fibers (tracheids) were peeled out using fine tweezers.<sup>20</sup> For the tensile test, the air-dried fibers were glued onto foliar frames, before mounting onto the crossheads of a tensile test device. The free length of the fiber was about 1 mm measured accurately before testing below a light microscope. The tensile apparatus was specially designed to measure mechanical properties under either wet or dry conditions and acquire spectra simultaneously. It consists of a dc-motor-driven high-resolution stage which permits a wide range of feed rates and a load (Honeywell/Sensotec, USA) cell with a capacity of 50 N (reproducibility better than 0.05%). Synchronized force and elongation data were recorded during the measurement. After tensile testing, one part of the broken fiber was dipped into liquid polyethylene glycol (PEG 2000, 60 °C). After solidification at room temperature, the stabilized fiber was cut below the fracture surface with a razor blade and rinsed in water (60 °C). From the cutting surface, images were taken in a low-vacuum mode with an environmental scanning electron microscope (Quanta 600FEG, FEI-Germany) to measure the cross-sectional area of the fiber cell wall for calculating the stress.

Spectra were acquired using a confocal Raman microscope (CRM200, WITTEC, Germany) equipped with an objective from Nikon (10 $\times$ , NA = 0.25) and a linear polarized laser (diode pumped Green laser,  $\lambda$  = 532 nm, CrystaLaser). The Raman light was detected by an air-cooled, back-illuminated spectroscopic CCD (ANDOR) behind a grating (600 g mm<sup>-1</sup>) spectrograph (ACTON). The electric vector of the laser was parallel to the fibers during tensile testing. To monitor molecular changes in plant cell walls simultaneously with straining required first of all an optimization of the acquisition (integration) time of the spectra along with the straining velocity. Integration time had to be long enough to get sharp Raman bands with a good signal-to-noise ratio to determine exactly band positions. However, short integration times were desired (i) to have no severe changes in stress and strain levels in the sample as well as in the focus position during one single spectrum acquisition and (ii) to get as many spectra as possible during one tensile test to reliably evaluate trends. With the finally chosen integration time of 30 s per spectrum and a straining velocity of 0.05  $\mu\text{m s}^{-1}$ , about 20 single Raman spectra with a good signal-to-noise ratio were collected during one single fiber test. Real-time spectra were monitored always before starting a new measurement (30 s), and when severe spectral changes were noticed, the fiber position and focal plane readjusted to get similar spectra. After the fiber ruptured, the same measurement position was looked for to acquire at the same fiber position a spectrum after failure. With the OPUS software package (version 5.5), band positions and heights were determined from the spectra without (data not shown) and after a 9-pt smoothing (Figure 1A, Figure 2, Figure 3A–B). For the band height determination, a baseline was drawn from 1177 to 1014  $\text{cm}^{-1}$  and the height at the two maxima around 1097 and 1127  $\text{cm}^{-1}$  measured to calculate the band height ratio (Figure 4).

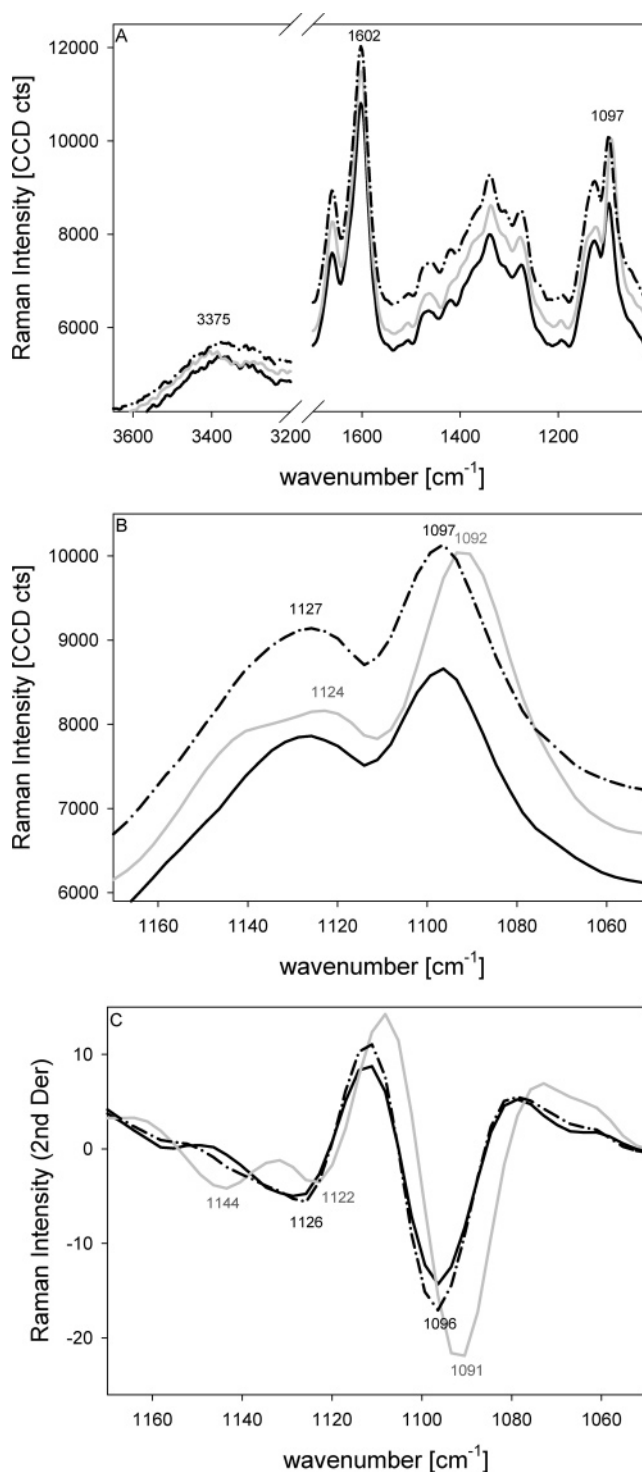


**Figure 1.** Single spectra (A) acquired in the beginning of the tensile test (black line), at a high stress/strain level (grey line) and after rupturing (dashed black line) showing the OH and the fingerprint region (A), the area from 1170 to 1050  $\text{cm}^{-1}$  (B), and the second derivatives (C).

Original spectra were also derived according to Savitzky and Golay<sup>22</sup> by means of a 9-pt smoothing filter and a second-order polynomial, followed by another 9-pt smoothing and searching for negative peaks to investigate band shifts derived from the second derivatives of the spectra (Figure 3C).

### Results and Discussion

The Raman spectrum of wood is rather complex due to its multicomponent nature. It is characterized by broad overlapping, CDV

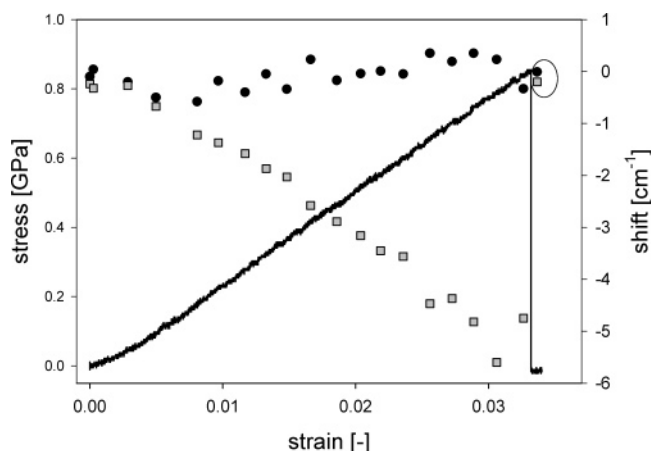


**Figure 2.** Stress–strain curve of a single spruce latewood fiber along with the calculated peak shift of the band at  $1097\text{ cm}^{-1}$  (gray squares) and  $1602\text{ cm}^{-1}$  (black circles).

often not clearly discernible bands (Figure 1A). Results from normal coordinate analyses of cellulose model compounds suggested that the vibrational motions of pure cellulose are already very complex and coupled.<sup>23</sup> The main features in the wood Raman spectra arise from cellulose and lignin, whereas the hemicelluloses have been found to contribute less.<sup>24</sup> The strongest band in our spectra was found around  $1602\text{ cm}^{-1}$  (Figure 1A), attributed to the aryl stretching of lignin.<sup>5</sup> Another strong, sharp band was detected around  $1097\text{ cm}^{-1}$ , deriving from CC and CO stretching of cellulose.<sup>5</sup> Three example spectra are shown, including a spectrum before straining (black line), at a high strain/stress level (gray line), and after the sample ruptured (black dashed line). Besides changes in the overall Raman intensity, some bands showed clear changes in band positions, e.g., the band at  $1097\text{ cm}^{-1}$  (Figure 1A,B). Another observed trend was a change of the maximum in the broad OH-stretching band from around  $3375\text{ cm}^{-1}$  to about  $3402\text{ cm}^{-1}$  during straining and back after rupturing (Figure 1A). A clear change in the hydrogen-bonding system during the linear elastic straining occurred, but unfortunately, the broadness due to the overlapping nature of this band together with the noise in this region (Figure 1A) allowed no detailed analysis. The band position in the OH-stretching region provides information about the presence and strength of hydrogen bonding. Bands originating from hydrogen-bonded O–H groups are shifted toward lower wavenumbers with respect to free O–H groups, and the stronger the hydrogen bond, the greater shift and intensity.<sup>25</sup> Therefore, a shift to higher wavenumbers might indicate that some hydrogen bonds are weakened during straining.

The main changes during tensile deformation of single normal spruce wood fibers were found in the C–C and C–O stretching region of the Raman spectra (Figure 1B,C) and OH region (Figure 1A). This is in accordance with results gained on different cellulosic materials studied by dynamic FT-IR spectroscopy.<sup>26</sup> They found that at the molecular level the strain distribution goes via the glucose ring, the C–O–C linkage between these rings, and the  $\text{O}(3)\text{H}\cdots\text{O}(5)$  intramolecular hydrogen bond.

Plotting the shift of the band position of every single spectrum (Figure 2, rectangles and circles) along with the stress–strain curve (black line) illustrates the progression during the tensile test. The spruce tracheid exhibited a linear elastic behavior and failed at an ultimate stress of  $0.85\text{ GPa}$  (Figure 2). Along with increasing stress and strain, the band at  $1097\text{ cm}^{-1}$  shifted remarkably to lower wavenumbers ( $1091\text{ cm}^{-1}$ ) (Figure 2, gray rectangles), whereas the band at  $1602\text{ cm}^{-1}$

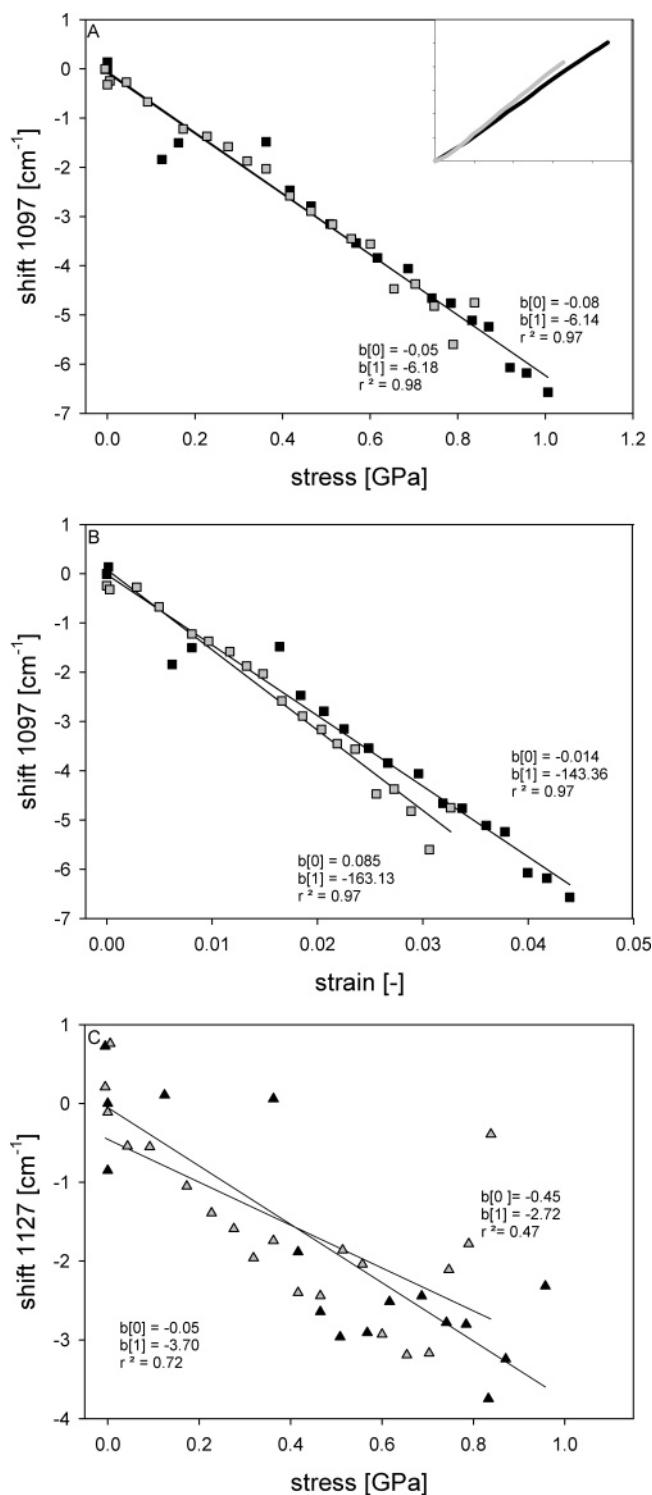


**Figure 3.** Correlation between the shift of the  $1097\text{ cm}^{-1}$  band (squares) and the applied stress (A) and strain (B) measured in two (black and gray) single-fiber tensile tests (stress–strain curves in the right insert). (C)  $1127\text{ cm}^{-1}$  band shift (triangle) calculated from the second derivatives of the spectra and correlated with stress.

stayed at one position (black circles). In the last spectrum before fiber rupture, at a strain level of  $0.033$  the  $1091\text{ cm}^{-1}$  band position did not further decrease but slightly increased. This was not observed in all other measurements (e.g., Figure 3A, black squares) and might be because the integration time of the last spectrum covered the failure event and exceeded  $10\text{ s}$  after the fiber had ruptured. With the released stress after failure, the band went back to its original position at  $1097\text{ cm}^{-1}$  (Figure



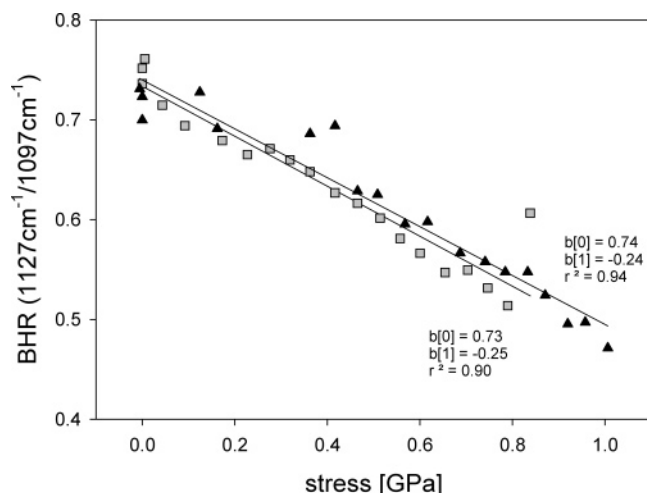


**Figure 4.** Band height ratio (BHR) calculated from the maximum intensities around 1097 and 1127  $\text{cm}^{-1}$  of the two measurements (black and gray) plotted together with the applied stress.

2, encircled area), which showed the elastic nature of this band shift.

The absence of a shift for the 1602  $\text{cm}^{-1}$  band was already reported by Eichhorn et al.<sup>13</sup> They concluded that lignin acts as a low-modulus, non-load-bearing amorphous polymer.<sup>13</sup> The shift of the band at 1095  $\text{cm}^{-1}$  was shown to monitor molecular stress in cellulosic fibers (cotton, flax, and hemp)<sup>13,18,19</sup> and also in wood slivers.<sup>13</sup> They found that for the tested cellulose fibers the shift rate is invariant with stress at a value of  $\sim 4.5 \text{ cm}^{-1}/\text{GPa}$ . Experiments on wood were done using a four-point-bending rig without force registration and thus included no relationship with stress, but only strain.<sup>13</sup> In our experiments on single wood fibers, the overall band shifts were quite high (5 to 7  $\text{cm}^{-1}$ ), and a shift rate of about  $6.1 \text{ cm}^{-1}/\text{GPa}$  was calculated from two repeated measurements (Figure 3A). The coefficient of determination between stress and peak shift was strong ( $r^2 = 0.97\text{--}0.98$ ), and the regression lines of the two measurements were exactly overlapping (Figure 3A). In the second measurement (black rectangles), higher stress and strain levels went hand in hand with higher band shifts ( $>5 \text{ cm}^{-1}$ , Figure 3A,B). The correlation of the band shift with strain was also high ( $r^2 = 0.97$ ), but the slope differed slightly between the two measurements (Figure 3B).

A band at about 1122  $\text{cm}^{-1}$ , assigned to the symmetric stretching of the COC in cellulose<sup>27</sup> and ring and C–O stretching modes,<sup>28</sup> was shown in flax and hemp fibers to shift to a similar extent as the 1097  $\text{cm}^{-1}$  band.<sup>19</sup> The broad band at about 1127  $\text{cm}^{-1}$  in the wood spectra (Figure 1A,B) is more superimposed by other bands than the one at 1097  $\text{cm}^{-1}$ .<sup>24</sup> The number of bands giving rise to the broad overlapping bands in the Raman spectrum is not known, which makes peak fitting particularly difficult. To enhance resolution and to improve the accuracy of the band position determination, the second derivatives (2nd Der) of the spectra were evaluated as well (Figure 1C). The second derivative is similar to the original spectrum in having peaks at roughly the same wavenumbers, although inverted in direction and additionally removing baseline differences. Applied to the wood spectra, e.g., the shoulder seen around 1144  $\text{cm}^{-1}$  in the spectra (Figure 1B) is discerned as a band and the broader band at about 1127  $\text{cm}^{-1}$  better resolved (Figure 1C). By determining the band positions from the 2nd Der, the calculated shifts of the 1097  $\text{cm}^{-1}$  band and its correlations with stress and strain remained the same, but were improved for the more superimposed 1127  $\text{cm}^{-1}$  band. In both

independent measurements, band positions showed variability, the correlation with stress was weaker than for the 1097  $\text{cm}^{-1}$  band, and the overall shift ( $-3 \text{ cm}^{-1}$ ) as well as the shift rate was cut to the half (Figure 3C). Besides, we noticed in both measurements a nonconcurrent decrease until sample rupture, but already an increase of about 0.1 GPa before the fiber failed (Figure 3C).

High variability was reported for the 1097  $\text{cm}^{-1}$  band shift in wood and was explained by the problem of focusing the laser spot onto one particular layer of the cell wall in four-point-bending tests.<sup>13</sup> Our measurement setup on single mechanically isolated wood fibers proved the very strong relationship of the shift of the band at 1097  $\text{cm}^{-1}$  with stress and strain with minor variability. However, evaluating the 1127  $\text{cm}^{-1}$  band revealed variability, which might to some extent be due to the problem of focusing and thus different superimposition with other components, e.g., lignin.

A closer look at the spectra before straining, at a high strain level, and after rupturing shows, besides the band shifts of the two discussed bands, also a changed band height ratio (Figure 1B). Calculating and plotting the intensity ratio of the 1127 and 1097  $\text{cm}^{-1}$  bands shows a linear course along with stress (Figure 4) and a going back after rupturing (not shown). The same intensity ratio was investigated in different cellulose fibers to follow molecular changes of the cellulose.<sup>25–29</sup> Besides cellulose composition and conformation, the ratio is also dependent on the alignment of the sample, if the laser light is polarized. The 1097  $\text{cm}^{-1}$  band becomes more intense when the cellulose molecules are aligned parallel to the electronic vector of the laser beam, compared to perpendicular alignment.<sup>28,30</sup> The 1126  $\text{cm}^{-1}$  band is not that sharp and well-resolved and might contain overlapping signals from hemicelluloses and lignin. In comparison to the 1097  $\text{cm}^{-1}$  band, the intensity does not change in relation to the fiber orientation, and thus, the changing ratio of the two bands can be used to follow changes in fiber orientation. The change in the ratio due to orientation was measured on the same fiber by gradually turning the fiber from parallel ( $0^\circ$ ) to perpendicular alignment ( $90^\circ$ ). The ratio changed gradually from 0.7 at parallel fiber alignment to 1.4 at perpendicular orientation (data not shown). During the straining of the fiber, we noticed a change of the ratio from 0.7 down to 0.5 (Figure 4), which might be interpreted as a continuous widening of the torsion angle of the glycosidic C–O–C bonding during straining and thus more parallel alignment of the C–O–C bonding.

## Conclusions

The reported methodical approach on micromechanical testing of single wood fibers along with simultaneous short-time acquisition of Raman spectra enabled us to follow molecular changes during straining. The short time acquisition and concurrent straining minimizes the effects of relaxation phenomena and allows in situ monitoring. Future experiments on native wood fibers (differing in chemical composition and cellulose orientation) and on chemically and enzymatically modified fibers will help to deepen the micromechanical understanding of plant cell walls and the associated macromolecules.

**Acknowledgment.** We thank Michaela Eder and Luna Goswami for isolation and preparation of single wood fibers, as well as determination of cross-sectional areas, and Dr. H. S. Gupta for help with the tensile test device.

## References and Notes

- (1) Page, D. H. A note on cell-wall structure of softwood tracheids. *Wood Fiber* **1976**, 7 (4), 246–248.
- (2) Jarvis, M. C.; McCann, M. C., Macromolecular biophysics of the plant cell wall: Concepts and methodology. *Plant Physiol. Biochem.* **2000**, 38 (1/2), 1–13.
- (3) Morris, V. J.; Ring, S. G.; MacDougall, A. J.; Wilson, R. H. Biophysical characterisation of plant cell walls. In *The Plant Cell Wall – Annual Plant Reviews*; Rose, J., Ed.; Blackwell Publishing, 2003; pp 55–91.
- (4) Agarwal, U. P.; Atalla, R. H. In-situ raman microprobe studies of plant cell walls – Macromolecular organization and compositional variability in the secondary wall of *Picea mariana* (Mill) Bsp. *Planta* **1986**, 169 (3), 325–332.
- (5) Agarwal, U. P. An Overview of Raman Spectroscopy as Applied to Lignocellulosic Materials. In *Advances in lignocellulosics characterization*; Argyropoulos, D. S., Ed.; TAPPI Press: Atlanta, GA, 1999; pp 209–225.
- (6) Schrader, B.; Klump, H. H.; Schenzel, K.; Schulz, H. Non-destructive NIR FT Raman analysis of plants. *J. Mol. Struct.* **1999**, 509, 201–212.
- (7) Fischer, S.; Schenzel, K.; Fischer, K.; Diepenbrock, W. Applications of FT Raman spectroscopy and micro spectroscopy characterizing cellulose and cellulosic biomaterials. *Macromol. Symp.* **2005**, 223, 41–56.
- (8) Atalla, R. H.; Agarwal, U. P. Raman microprobe evidence for lignin orientation in the cell walls of native woody tissue. *Science* **1985**, 227, 636–638.
- (9) Gierlinger, N.; Schwanninger, M. Chemical imaging of poplar wood cell walls by confocal Raman microscopy. *Plant Physiol.* **2006**, 140, 1246–1254.
- (10) Mitra, V. K.; Risen, W. M. J. A laser Raman study of the stress dependence of vibrational frequencies of a monocrystalline polydiacetylene. *J. Chem. Phys.* **1977**, 66 (6), 2731–2736.
- (11) Davies, R. J.; Eichhorn, S. J.; Riekel, C.; Young, R. J. Crystal lattice deformation in single poly(*p*-phenylene benzobisoxazole) fibres. *Polymer* **2004**, 45 (22), 7693–7704.
- (12) Yeh, W.-Y.; Young, R. J., Molecular deformation processes in aromatic high modulus polymer fibres. *Polymer* **1999**, 40, 857–870.
- (13) Eichhorn, S. J.; Sirichaisit, J.; Young, R. J. Deformation mechanisms in cellulose fibres, paper and wood. *J. Mater. Sci.* **2001**, 36, 3129–3135.
- (14) Eichhorn, S. J.; Young, R. J.; Davies, R. J.; Riekel, C. Characterisation of the microstructure and deformation of high modulus cellulose fibres. *Polymer* **2003**, 44 (19), 5901–5908.
- (15) Eichhorn, S. J.; Young, R. J.; Davies, G. R. Modeling crystal and molecular deformation in regenerated cellulose fibers. *Biomacromolecules* **2005**, 6 (1), 507–513.
- (16) Kong, K.; Eichhorn, S. J. Crystalline and amorphous deformation of process-controlled cellulose-II fibres. *Polymer* **2005**, 46 (17), 6380–6390.
- (17) Kong, K.; Eichhorn, S. J. The influence of hydrogen bonding on the deformation micromechanics of cellulose fibers. *J. Macromol. Sci., Phys.* **2005**, B44 (6), 1123–1136.
- (18) Eichhorn, S. J.; Young, R. J. Deformation micromechanics of natural cellulose fibre networks and composites. *Compos. Sci. Technol.* **2003**, 63 (9), 1225–1230.
- (19) Eichhorn, S. J.; Hughes, M.; Snell, R.; Mott, L. Strain induced shifts in the Raman spectra of natural cellulose fibers. *J. Mater. Sci. Lett.* **2000**, 19 (8), 721–723.
- (20) Burgert, I.; Keckes, J.; Frühmann, K.; Fratzl, P.; Tschegg, S. E. A comparison of two techniques for wood fibre isolation- evaluation by tensile tests on single fibres with different Microfibril angle. *Plant Biol.* **2002**, 4, 9–12.
- (21) Burgert, I.; Gierlinger, N.; Zimmermann, T. Properties of chemically and mechanically isolated fibres of spruce (*Picea abies* [L.] Karst.). Part I: Structural and chemical characterisation. *Holzforschung* **2005**, 59 (2), 240–246.
- (22) Savitzky, A.; Golay, M. J. E. Smoothing and differentiation of data by simplified least squares procedures. *Anal. Chem.* **1964**, 36, 1627–1639.
- (23) Cael, J. J.; Gardner, K. H.; Koenig, J. L.; Blackwell, J. Infrared and Raman spectroscopy of carbohydrates. Paper V Normal coordinate analysis of cellulose I. *J. Chem. Phys.* **1975**, 62 (3), 1145–1153.
- (24) Agarwal, U. P.; Ralph, S. FT-Raman Spectroscopy of Wood: Identifying Contributions of Lignin and Carbohydrate Polymers in the Spectrum of Black Spruce (*Picea mariana*). *Appl. Spectrosc.* **1997**, 51 (11), 1648–1655.
- (25) Marechal, Y.; Chanzy, H. The hydrogen bond network in I-beta cellulose as observed by infrared spectrometry. *J. Mol. Struct.* **2000**, 523, 183–196.
- (26) Hinterstoisser, B.; Akerholm, M.; Salmen, L. Load distribution in native cellulose. *Biomacromolecules* **2003**, 4 (5), 1232–1237.
- (27) Edwards, H. G. M.; Farwell, D. W.; Webster, D. FT Raman microscopy of untreated natural plant fibres. *Spectrochim. Acta, Part A* **1997**, 53 (13), 2383–2392.
- (28) Wiley, J. H.; Atalla, R. H. Band assignment in the raman spectra of celluloses. *Carbohydr. Res.* **1987**, 160, 113–129.
- (29) Jähn, A.; Schröder, M. W.; Fütting, M.; Schenzel, K.; Diepenbrock, W. Characterization of alkali treated flax fibres by means of FT-Raman spectroscopy and environmental scanning electron microscopy. *Spectrochim. Acta, Part A* **2002**, 58 (10), 2271–2279.
- (30) Sturcova, A.; Davies, G. R.; Eichhorn, S. J. Elastic modulus and stress-transfer properties of tunicate cellulose whiskers. *Biomacromolecules* **2005**, 6 (2), 1055–1061.

BM060236G